Silicon Nitride Nanosieve Membrane

ARTICLE *in* NANO LETTERS · FEBRUARY 2004

Impact Factor: 13.59 · DOI: 10.1021/nl0350175

NANO LETTERS

2004
Vol. 4, No. 2
283−287

Silicon Nitride Nanosieve Membrane

Hien D. Tong,* Henri V. Jansen, Vishwas J. Gadgil, Cazimir G. Bostan, Erwin Berenschot, Cees J. M. van Rijn, and Miko Elwenspoek

MESA+ Research Institute, University of Twente, P.O. Box 217, 7500 AE Enschede, The Netherlands

Received November 12, 2003; Revised Manuscript Received December 15, 2003

ABSTRACT

An array of very uniform cylindrical nanopores with a pore diameter as small as 25 nm has been fabricated in an ultrathin micromachined silicon nitride membrane using focused ion beam (FIB) etching. The pore size of this nanosieve membrane was further reduced to below 10 nm by coating it with another silicon nitride layer. This nanosieve membrane possesses adequate mechanical strength up to several bars of transmembrane pressure, and it can withstand high temperatures up to 900 °C. In addition, it is inert to many aggressive chemicals such as hot concentrated potassium hydroxide (KOH), piranha ($H_2SO_4 + H_2O_2$), and nitric acid (HNO_3).

The development of fluid-separation membranes started almost one century ago with research on liquid filtration, and in past decades, their use in gas-separation units has been studied as well. In the beginning, these membranes consisted almost exclusively of a relatively thick layer (several micrometers) of nanoporous organic or inorganic material with nonuniform perforations and random pore diameters. Despite the success of nanoporous membranes in liquid filtration and gas separation, the selectivity and strength of the membranes are limited by the fairly broad pore-diameter distribution.[1] However, a nanomembrane with perforations essentially of one size and cylindrical pore shape will have many potential applications, such as absolute sterile filtration (bacteria as well as viruses), size-exclusion-based separations,[1−4] templates for nanosensors,[5] and masks for stencils.[6] Depending on the specific application, bio- or blood-compatible materials should be used for the construction of the uniformly perforated membrane. Moreover, in most applications there is a need for nanoporous layers having adequate mechanical strength with respect to transmembrane pressure, low flow resistance to enable high flux, and sufficient thermal and chemical stability in harsh environments. Nanoporous membranes with arrays of cylindrical pores and uniform pore sizes between several tens down to below 10 nm will be called nanosieves in the following discussion.

Two types of nanosieves can be distinguished. The first kind uses a layer that is relatively thick with respect to the pore diameter so that an array of nanochannels is created through the layer.[2,4] The second kind uses a membrane having a thickness on the order of or even smaller than the diameter of the nanopore so that the pores closely resemble an array of nanoholes inside the membrane. An interesting application for such an array of nanoholes is that fluid can be filtered against larger particles with a relatively high flux in comparison with an array of nanochannels. Nevertheless, for identical pore diameters, the nanochannel type has the advantage over the nanohole type of being mechanically more robust but has the disadvantage of having a much higher flow resistance. In this paper, a technique is presented that combines the advantages of both techniques (i.e., a strong nanosieve membrane with a high throughput).

The nanopores are often machined in a suspended low-stress silicon nitride (SiN) membrane[1,5−10] for several reasons, such as the availability of SiN membranes after standard microsystem processing such as KOH etching of a silicon support and the thermal stability and chemical inertness of SiN material. So far, electron beam lithography followed by reactive ion etching (RIE)[5,6] or FIB etching [7−10] have been used to create pores in the SiN membrane. Because the suspended SiN membrane should survive handling during the fabrication process and application, its thickness should be made adequate. However, the relatively thick membrane renders the creation of small pores because of the difficulty of etching pores with high aspect ratios. In the case of direct pore drilling by FIB, the beam diameter and especially the relative thickness of the SiN membrane limit pore diameters to 50 nm or greater.[7−10]

Recently, several techniques have been developed to reduce the size of the previously FIB-drilled nanopores, but their applications for many pores are difficult[10] or time-consuming.[11] However, a simple strategy to drill small pores directly by FIB is to reduce the thickness of the SiN membrane. Of course, it needs to be done without noticeably sacrificing the strength and perforated area of the membrane. Here we report the fabrication of strong SiN nanosieve

* To whom correspondence should be addressed. E-mail: T.Hien@el.utwente.nl. Phone: +31 53 489 2805. Fax: +31 53 489 3343.

10.1021/nl0350175 CCC: $27.50
Published on Web 01/13/2004

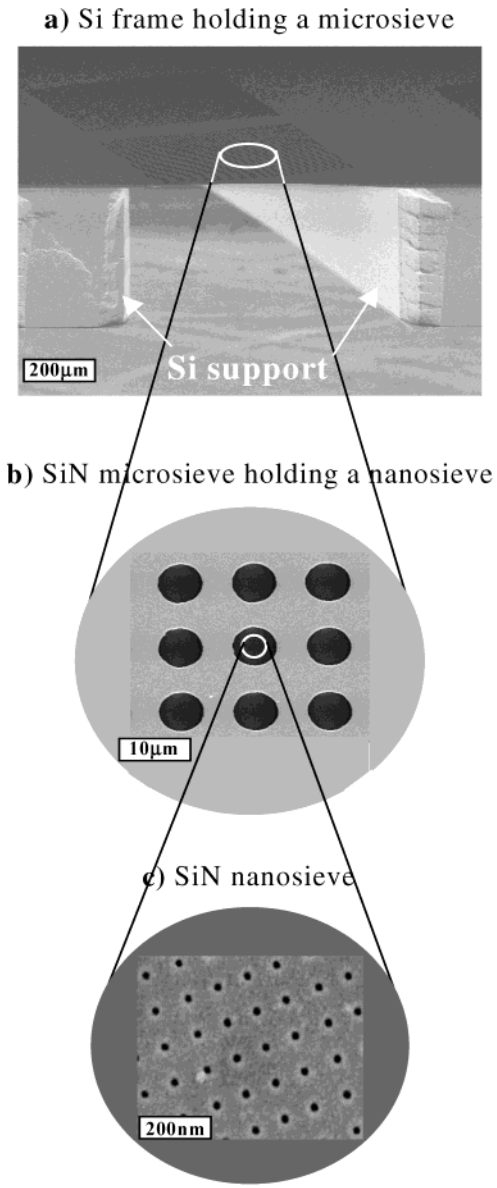

Figure 1. SEM overview with close-ups of the nanosieve membrane. (a) A strong, thick silicon frame supports a thin SiN microsieve. (b) This microsieve supports a nanosieve. (c) The nanosieve.

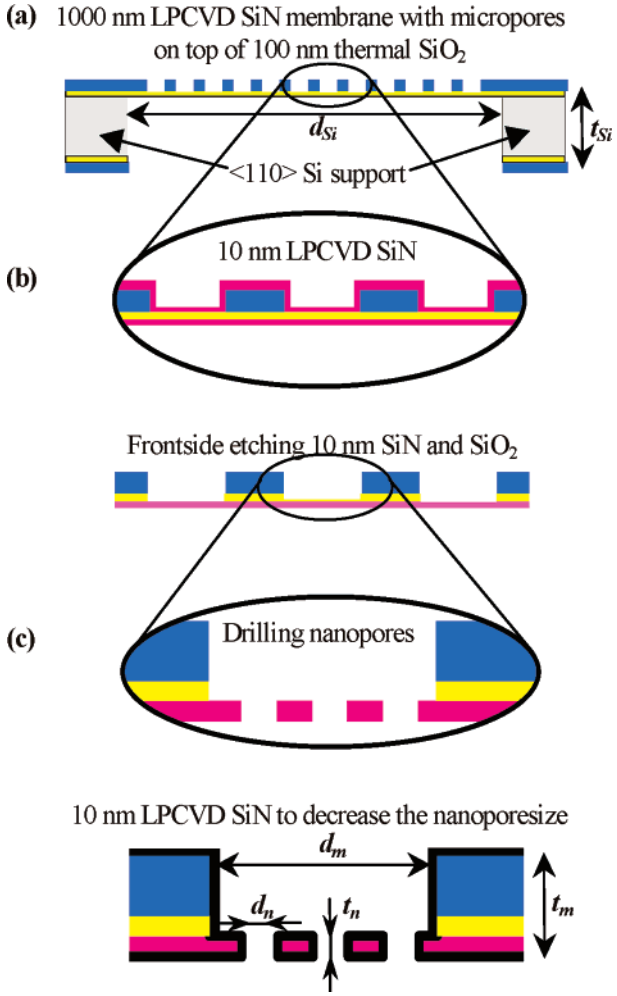

Figure 2. Simplified process flow of the nanosieve membrane. (a) A ⟨110⟩ silicon frame is etched with KOH to support a 1000-nm thin SiN microsieve on top of a 100-nm thin SiO_2 membrane. (b) This microsieve consists of an array of 5-μm circular perforations etched with RIE to support a 10-nm thin SiN nanomembrane. (c) This nanomembrane is etched with FIB with an array of nanopores forming the nanosieve.

membranes with a small and uniform pore size. The essence of the method is the micromachining of an ultrathin nanosieve within a thin supporting microsieve using FIB with the smallest possible beam current to drill the holes. In this way, uniform pores as small as 25 nm were drilled.

Figure 1 is an overview of the nanosieve membrane, and Figure 2 shows its simplified process flow. The process starts with a microsieve supported by a ⟨110⟩ silicon frame (Figures 1a and 2a), for which its detailed fabrication process has been reported earlier.[12] This microsieve is conformally coated with 10-nm SiN by means of low-pressure chemical vapor deposition (LPCVD)[13] as shown in Figure 2b. However, this layer is removed from the top of the microsieve support by dry RIE using a CHF_3/O_2 mixture. Subsequently, a wet buffered hydrofluoric acid (BHF) etching of the sacrificial SiO_2 results in a structure that has a 10-nm thin SiN membrane supported by the microsieve (Figure 2b). Finally, a dual FIB system (FEI Inc. FIB 200) with a 30-KV gallium beam is used to drill the pores in the nanomembrane, and the nanosieve is formed (Figure 2c). Before the FIB procedure, the samples were coated with 2 nm of chromium (Cr) to reduce charging during exposure to electron and ion beams. The smallest possible FIB current of 1 pA is used because such a current has a small beam diameter (ca. 10-nm fwhm corresponding to a current density of ca. 1.2 A/cm^2) and a narrow beam-diameter distribution (uniform pores).[14,15] The FIB process is controlled by a Matlab program, which digitally and repetitively scans the ion beam to make an array of pores with a dwell time of 10 μs.

Figure 3a is a high-resolution scanning electron microscopy image (HRSEM: LEO Gemini 1550, 2-nm lateral resolution) of the nanopores. As shown, the pores are circular with diameters of around 25 nm and a pore pitch of around 115 nm. The drilled pores are uniform in size (<10% variation) over the whole 50 × 50 μm^2 patterned area. As discussed above, using a small ion beam current did enable

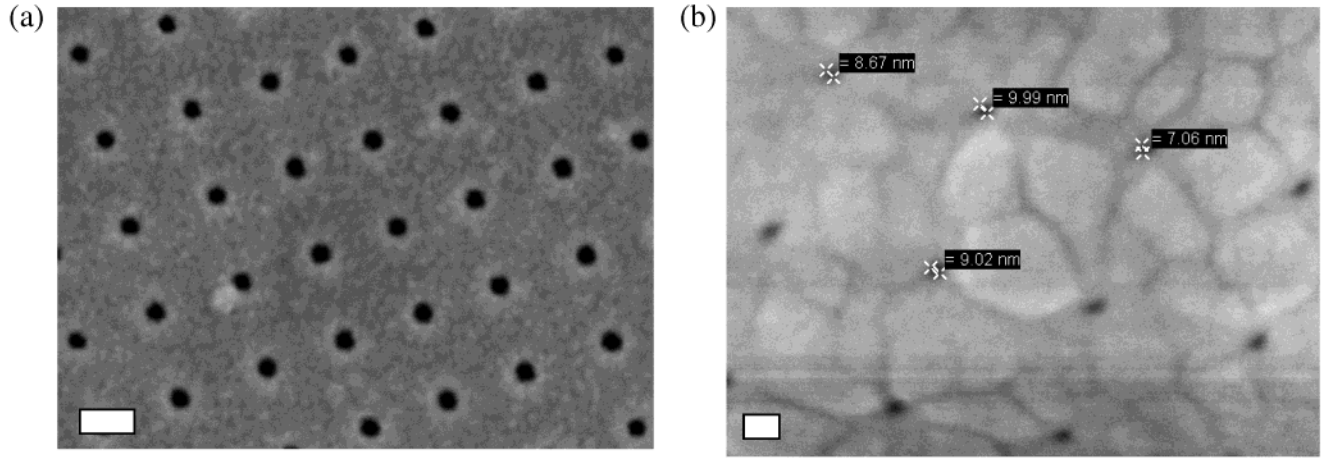

Figure 3. (a) Nanopores, 25 nm in diameter, were directly drilled by FIB in a 10-nm SiN membrane (110 Kx, scale bar: 50 nm). (b) Pores with sizes below 10 nm were obtained by coating the 25-nm pores with 10-nm LPCVD SiN (150 Kx, scale bar: 20 nm).

the creation of such small pores with high uniformity. Moreover, although the smallest current was used, the drilling time is still short due to drilling through an ultrathin layer. HRSEM images were taken from both sides of the membrane, revealing that there is almost no difference between the top and bottom pore diameters. This indicates that the pore wall has a slope angle of nearly 90° with respect to the lateral direction, which is consistent with the reported work that used small FIB currents.[15]

To obtain even smaller pores, the FIB-drilled pores are coated with another ultrathin layer of LPCVD SiN. Prior to the coating, the samples were treated in oxygen plasma to remove hydrocarbon contaminants from FIB and SEM procedures, followed by the removal of Cr in a Cr etching solution; the samples were finally cleaned in deionized water. Using LPCVD again, we found that SiN has the advantage of minimizing stress due to thermal mismatch. Moreover, it exhibits conformal step coverage and high uniformity and completely covers the membrane unit.[13] The initial pores of around 25 nm (shown in Figure 3a) were coated with 10-nm SiN at a deposition rate of 0.13 nm/s, and the HRSEM image of the coated pores is shown in Figure 3b; all of the pores are now below 10 nm in size.

Important characteristics to categorize fluidic sieves are the permeability, strength, and selectivity. The permeability describes the ability of the sieve to achieve a high throughput, and the strength describes the ability of the sieve to withstand a certain flux without breaking. Finally, the selectivity describes the ability of the sieve to separate the desired component from the feed mixture. Next, the viscous fluidic transport through the nanosieve will be discussed, and after that, we will discuss the molecular transport of gas molecules.

For viscous laminar flow at sufficiently small Reynolds number (Stokes or creeping flow) for a fluid medium with viscosity μ [Pa·s] through a circular opening with radius r [m] in an infinitely thin wall, the pressure difference Δp is proportional to the volume flow rate Φ_V [m^3/s] as $\Delta p = \Phi_V \cdot (3\mu/r^3)$.[19] However, for a wall with a finite thickness t, the equation is altered because of frictional losses with the walls with a correction factor of $C(t, r) = (1 + (8 \cdot t)/(3\pi \cdot r)) \approx (1 + (0.85 \cdot t)/(r))$.[20] Moreover, in the case of an array of pores, the fluid flow in one pore will influence the flow in its neighboring pores. For a nanosieve with a square array of apertures and a fraction χ of perforated area, the correction is given by $C(\chi) = 1 - 0.344 \cdot \chi^{3/2} - 0.111 \cdot \chi^{5/2} - 0.066 \cdot \chi^{7/2} \approx 1 - 0.34 \cdot \chi^{3/2}$ for $\chi < 20\%$.[21] Finally, for higher laminar flow rates an additional pressure drop will arise just before the entrance of the pores, resulting in a quadratic component to account for this nonviscous kinetic loss.[22] All of the above-mentioned effects were combined by van Rijn and Elwenspoek.[1]

$$\Delta p = \Phi_V \cdot \left(\frac{3\mu}{r^3}\right) \cdot \left(1 + \frac{0.85 \cdot t}{r}\right) \cdot (1 - 0.34 \cdot \chi^{3/2}) + \Phi_V^{\,2} \cdot \left(\frac{\rho}{4\pi^2 \cdot r^4}\right) \text{[Pa]} \quad (1)$$

where ρ [kg/m^3] is the mass density of the fluid medium. For water, $\rho = 998.2$ kg/m^3 and $\mu = 1.00 \times 10^{-3}$ Pa · s at 293 K. ($\rho = 997.0$ kg/m^3 and $\mu = 0.89 \times 10^{-3}$ Pa · s at 298 K.) Assuming an array of pores with 10-nm radius and 10-nm membrane thickness (i.e., $C(t, r) = 1.85$), a pore pitch of 100 nm (i.e., a density of 10^{14} pores/m^2 and a perforated fraction of 3% giving $C(\chi) = 0.995$), and neglecting kinetic losses, a transmembrane pressure of ca. 1 bar ($= 10^5$ Pa) is calculated for a water flux of 2 L/m^2 s. Unfortunately, the number of nanopores is limited by the FIB system used in this study to less than 1 million, thus limiting the water flux for a nanosieve to 2×10^{-8} L/s. The kinetic losses become prominent when $\Phi_V \geq 10^{-4} \cdot r = 10^{-12}$ m^3/s, which is 10^5 times the flux in the single nanopore; therefore, the kinetic losses are indeed negligible.

To calculate the transmembrane pressure across the nanosieve for a certain flux of gas molecules, the mean free path λ of the molecule with respect to the pore diameter of the nanomembrane d_n is important. Following Knudsen's theory, when $d_n > \lambda/100$ many gas−gas collisions take place during transport through the orifice and the calculations closely resemble Stokes viscous flow as discussed before. However, when $d_n < \lambda$ the flow is molecular, meaning that

only a few intermolecular collisions occur during transport through the membrane and the flow is limited by collisions with the walls. Therefore, for molecular gas transport the analysis of the flow is primarily a geometrical problem of determining the total open area and restrictive effect of the walls on the free flight of a molecule. Now, when two compartments are separated using a membrane with very small pores, the rate of escape through the membrane is equal to the rate at which the gas molecules strike the area of the pore. Therefore, if the area of the pore is $A = \pi r^2$ and the molar number of molecules that escape per unit time is Φ_M [mol/s], then the transmembrane pressure can be calculated as $\Delta p = \Phi_M \cdot (\sqrt{2\pi MRT}/\pi r^2)$.[16] M is the molar mass [kg/mol] of the gas, R is the universal gas constant [J/mol K], and T is the absolute temperature [K]. The fact that this number is proportional to $1/\sqrt{M}$ is the origin of Graham's law of effusion—the rate of effusion is inversely proportional to the square root of the molar mass M. Furthermore, the molecular flow resistance of a pore is caused by the random reflection of a low-energy molecule against the sidewall. Therefore, there is only a limited change for a molecule to enter the pore with radius r and height t (Figure 2c). This correction depends on the aspect ratio $AR = t/r$ and is known as the Clausing factor $C \approx (1 + (0.46 \cdot t)/(r))^{-1}$.[16]

$$\Delta p = \Phi_M \cdot \left(\frac{\sqrt{2\pi MRT}}{\pi r^2}\right) \cdot \left(1 + \frac{0.46 \cdot t}{r}\right) \text{[Pa]} \qquad (2)$$

A similar equation holds for molecular flow in the nanopore with $AR_n = t_n/r_n$ as well as in the micropore with $AR_m = t_m/r_m$. For gases, the mean free path is inversely proportional to pressure and is typically around 70 nm at a pressure of 1 bar. This is much larger than the thickness of the membrane in this study; therefore, the flow is treated molecularly. Using the same sieve as in the example for viscous fluid flow with $M = 0.032$ kg/mol for oxygen, $R = 8.3$ J/mol K, and $T = 293$ K, a pressure drop of ca. 1 bar occurs for a gas flux of 90 mol/m^2 s, which resembles 2000 L/m^2 s; when the number of pores is limited to 1 million, this means a flux of 90×10^{-8} mol/s.

The mechanical strength of the nanosieve membrane is an important characteristic because of the fact that a high transmembrane flux will cause a high transmembrane pressure drop. The maximum transmembrane pressure ΔP_{max} before a membrane with radius r_m and thickness t_n (see Figure 2c) breaks may be predicted as[17]

$$\Delta P_{max} = 0.29 \cdot K \cdot \left(\frac{t_n}{r_m}\right) \cdot \sigma_{yield} \cdot \sqrt{\frac{\sigma_{yield}}{E}} \qquad \text{[Pa]} \quad (3)$$

σ_{yield} is the yield stress, E is Young's modulus of the membrane material, and K is the nonperforated fraction of the membrane. Setting $\sigma_{yield} = 4 \times 10^9$ Pa and $E = 385 \times 10^9$ Pa for SiN, $r_m = 2.5$ μm, $t_n = 0.01$ μm, and $K = 0.8$; $\Delta P_{max} = 3.8$ bar is calculated for the fabricated nanosieve membrane. This is close to the rupture strength of $P_{max} = 2 \pm 0.2$ bar as found experimentally.[17] Equation 3 can be used in optimizing the dimensions of both the microsieve with respect to the silicon frame (d_{Si}, t_m) and the nanosieve with respect to the microsieve support (d_m, t_n). With respect to the ultrathin nanomembrane, it is important to notice that the layer is deposited in such a way that an atomically smooth and planar surface is guaranteed. Such extremely smooth and planar surfaces increase the strength of the membrane and exhibit a further downscaling of the membrane's thickness.

It should be noted that the hydrodynamic calculation above (eq 1) does not include the effect of electroviscous forces due to the electric double layer positioned at the interface of a fluid with the membrane surface. Electroviscous forces can be comparable to and in some cases larger than the hydrodynamic forces.[23,24] Moreover, the stick−slip flow transition, depending on the geometry and surface properties of the membrane material, may play a dominant role.[25] However, until now these effects have been studied only for relatively long channels, and more experimental data is needed to test the non-hydrodynamic behavior of the nanosieve membrane. Also, the calculation concerning molecular flow (eq 2) is not aimed at applications where the gas mixture is separated with respect to molecular sizes. However, the separation of gases by nanosieve membranes with a pore diameter below 1 nm may be similar to that of silica and zeolite membranes, which was thoroughly described by Burggraaf and Cot.[26] Moreover, for low-flow conditions, the effects of leakage and outgassing may become very prominent and need appropriate attention. Nevertheless, the hydrodynamic calculations are very useful in applications concerning ultrafiltration. In filtration, generally a number of larger molecules, viruses, or gas bubbles should be separated from a fluidic medium. In such cases, the exact absolute value of the flux is less important as long as all of the "unwanted" particles are filtered out completely. This is especially important in applications concerning sterile filtration.

Experimentally, it is found that the chemical stability of the fabricated sieves is excellent; no change in the pore size is observed after dipping the membranes into aggressive solutions such as hot concentrated KOH (25% at 75 °C), piranha ($H_2SO_4/H_2O_2 = 3/1$ mixture at 100 °C), or $HN0_3$ (69% at 95 °C). Each test was conducted for 30 min. This property allows the nanosieves to be used in most separation environments and makes cleaning easy. In addition, the nanosieves survived at temperatures of up to 900 °C, allowing them to be used in harsh environments where any known polymeric membrane would fail.[3]

The fabricated nanosieve membranes may be used for various size-exclusion-based separations in bioseparation and nanomedicine[1−4] with the advantage of gaining high separation fluxes or improving dynamic responses of the process because of the drastic reduction in membrane thickness—10 to 30 nm for the present membranes compared to 9 μm for the microfabricated channel pores [2,4] and 100−200 μm for the polymeric membranes.[3] Additionally, the present membrane may be used as a shadow mask for stencils,[5] or it may be integrated with other silicon-based components such as nanochannels[18] or nanopumps to set up innovative applications.

In summary, ultrathin SiN nanosieve membranes with uniform cylindrical pores and a pore size down to below 10 nm have been demonstrated. In addition, these nanosieve membranes possess adequate mechanical strength, possible high separation flux, and high chemical and thermal stability. These properties allow them to be used in numerous of applications in different sectors.

Acknowledgment. We are grateful for financial support from STW (the Dutch Technology Foundation, STW-PROJECT EST48) and thank Rik de Boer, Mark Smithers, and Bert Otter for technical support.

References

(1) Rijn, C. J. M.; Elwenspoek, M. *IEEE Conf. MEMS'95*, 1995; pp 83−87.
(2) Freitas, R. A. *Stud. Health Techn. Infor.* **2002**, *80*, 45−59.
(3) Mulder, M. *Basic Principles of Membrane Technology*; Kluwer Academic Publishers: Norwell, MA, 1998.
(4) Desai, A. T.; Hansford, D. J.; Kulinsky, L.; Nashat, A. H.; Rasi, G.; Tu, J.; Wang, Y.; Zhang, M.; Ferrari, M. *Biomed. Microdevices* **1999**, *2*, 11−40.
(5) Chen, J.; Reed, M. A.; Rawlett, A. M.; Tour, J. M. *Science* **1999**, *286*, 1550−1552.
(6) Deshmukh, M. M.; Ralph, D. C.; Thomas, M.; Silcox, J. *Appl. Phys. Lett.* **1999**, *75*, 1631−1633.
(7) Schmidt, C.; Mayer, M.; Vogel, H. *Angew. Chem., Int. Ed.* **2000**, *39*, 3137−3140.
(8) Geoch, J. E. M.; McGeoch, M. W.; Carter, D. J. D.; Schuman, R. F.; Guidotti, G. *Med. Bio. Eng. Comp.* **2000**, *38*, 13−119.
(9) Schenkel, T.; Radmilovic, V.; Stach, E. A.; Park, S. J. Persaud, A. *International Conference on Electron, Ion and Photon Beam Technology and Nanofabrication*, 2003.
(10) Li, J.; Stein, D.; McMullan, C.; Branton, D.; Azis, M. J.; Golovchenko, J. A. *Nature* **2001**, *412*, 166−169.
(11) Storm, A. J.; Chen, J. H.; Ling, X. S.; Zandbergen, H. W.; Dekker, C. *Nat. Mater.* **2003**, *2*, 537−540.
(12) Tong, H. D.; Gielens, F. C.; Hoang, H. T.; Berenschot, J. W.; De Boer, M. J.; Gardeniers, J. G. E.; Jansen, H. V.; Nijdam, W.; Rijn, C. J. M.; Elwenspoek, M. *IEEE Transducers'03*, 2003; pp 1742−1745.
(13) Gardeniers, J. G. E.; Tilmans. H. A. C. *J. Vac. Sci. Technol., A* **1996**, *14*, 2879−2892.
(14) Harriott, L. R. *J. Vac. Sci. Technol., B* **1993**, *11*, 2012−2015.
(15) Lipp, S.; Frey, L.; Franz, G.; Demm, E.; Petersen, S.; Ryssel, H. *Nucl. Instrum. Methods Phys. Res., Sect. B* **1995**, *106*, 630−635.
(16) Elwenspoek, M. C.; Jansen, H. V. *Silicon Micromachining*; Cambridge University Press: Cambridge, England, 1998; pp 216−355.
(17) Rijn, C. J. M.; Wekken, M.; Nijdam, W.; Elwenspoek, M. *J. Microelectromech. Syst.* **1997**, *6*, 48−54.
(18) Craighead, H. G. *Science* **2000**, *290*, 1532−1535.
(19) Sampson, R. A. *Philos. Trans. R. Soc. London, Ser. A* **1891**, *182*, 449−518.
(20) Dagan, Z.; Weinbaum, S.; Pfeffer, R. *Chem. Eng. Sci.* **1983**, *38*, 583−596.
(21) Tio and Sadhal. *Appl. Sci. Res.* **1994**, *52*, 1−20.
(22) Michel, S. J. *Fluid and Particle Mechanics*; Pergamon Press: Oxford, England, 1970; pp 101−102.
(23) Vainshtein, P.; Gutfinger, C. *J. Micromech. Microeng.* **2002**, *12*, 252−256.
(24) Huisman, I. H.; Trägårdh, G. Trägårdh, C.; Pihlajamäki, A. *J. Membr. Sci.* **1998**, *147*, 187−194.
(25) Cheikh, C. and Koper, G. *Phys. Rev. Lett.* **2003**, *91*, 156102-1/4.
(26) Burggraaf, A. C.; Cot, L. *Fundamentals of Inorganic Membrane Science and Technology*; Elsevier: Amsterdam, 1996; pp 374−386.

NL0350175